

Asymmetric Transfer Hydrogenation

Novel Chiral PNNP Ligands with a Pyrrolidine Backbone – Application in the Fe-Catalyzed Asymmetric Transfer Hydrogenation of Ketones

Elisabet Mercadé,^[a] Ennio Zangrando,^[b] Anna Clotet,^[a] Carmen Claver,^{*,[a,c]} and Cyril Godard^{*,[a]}

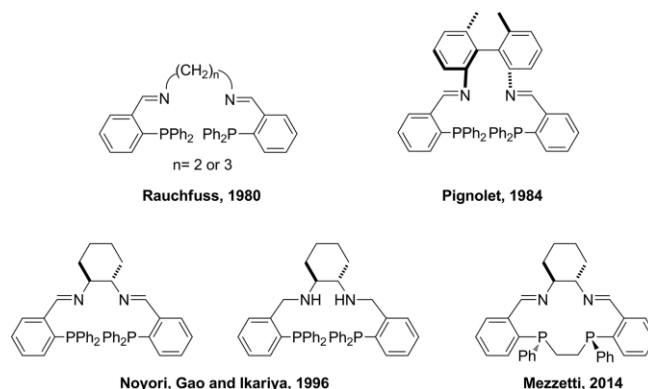
Abstract: The PNNP ligand (*R,R*)-[PPh₂(2-C₆H₄)CH=N(pyrrolidine-NBn)-]₂ **2** was prepared by condensation between 2-diphenylphosphino benzaldehyde and the pyrrolidine-substituted diamine **1**. Reduction with NaBH₄ in MeOH afforded (*R,R*)-{PPh₂(2-C₆H₄)CH-NH(pyrrolidine-NBn)-}₂ **3**. The corresponding iron(II) complexes [FeCl₂(**2**)] (**4**), [Fe(CH₃CN)₂(**2**)](BF₄)₂ (**5**) and [Fe(CH₃CN)₂(**2**)](PF₆)₂ (**6**) were synthesized and fully character-

ized by NMR, ESI-HRMS, and EA. DFT calculations for complexes [FeCl₂(**2**)] (**4**) and [Fe(CH₃CN)₂(**2**)](BF₄)₂ (**5**) were carried out in order to investigate the stability of related structures. The PNNP ligands **2** and **3** in combination with Fe₃(CO)₁₂ as iron source were tested as catalysts in the asymmetric transfer hydrogenation of a variety of ketones with conversions higher than 95 % and enantioselectivities up to 97 %.

Introduction

Homogeneous catalyst progress has traditionally focused on the second- and third-row transition metals in combination with simple ligands.^[1] In general, these catalysts provide high turnover frequencies (TOF) and product selectivities which are difficult to achieve by the less active first-row transition metals.^[2] However, the limited availability of precious metals as well as their high price and toxicity diminishes their attractiveness and make desirable the search of more sustainable and economically friendly alternatives.^[3]

Chiral tetradentate ligands offer a great advantage in catalysis due to their conformational and configurational rigidity arising from their chelation.^[4,5] The first achiral tetradentate ligand containing a N₂P₂ donor scaffold was described by Rauchfuss and co-workers in 1980.^[6] Later, Pignolet and co-workers reported the chiral version using the 2,2'-dimethyl-6,6'-diaminobiphenyl as the chiral framework and its coordination to Rh(I) and Ir(I).^[5] However, the most important breakthrough was carried out by Noyori, Gao and Ikariya in 1996, effectively applying Ru-PNNP complexes in the asymmetric transfer hydrogenation of ketones.^[7] Recently, Mezzetti and co-workers prepared chiral macrocyclic N₂P₂ ligands containing two stereogenic phosphorus donor atoms and their related Fe(II) complexes (Scheme 1).^[8]

Scheme 1. Selected PNNP and macrocyclic N₂P₂ ligands.

In 2010, Beller and co-workers reported the use of a chiral PNNP ligand with [Et₃NH][HFe₃(CO)₁₁] as iron source for the asymmetric transfer hydrogenation of ketimines with enantioselectivities up to 98 %.^[9] The group of Morris and co-workers also developed a series of well-defined chiral Fe(II)-PNNP complexes which provided high activities and enantioselectivities for the asymmetric transfer hydrogenation of C=O^[10] and C=N^[11] bonds.^[12]

Modification in the diamine^[13] backbone and the phosphine^[14] framework lead to fine tuning of the properties of these catalysts (Scheme 2). The complex [Fe(CH₃CN)(CO)(A)]-(BF₄)₂, also indicated as *first generation*, reduces acetophenone with 63 % enantioselectivity and a TOF of 1600 h⁻¹.^[10] Later, it was demonstrated that this type of complexes form metallic nanoparticles under catalytic conditions.^[15] Complexes [Fe(Br)(CO)(B/C)](BPh₄), which constitute the *second generation*, hydrogenate acetophenone with ee's up to 90 % with TOF's of 30000 and 26000 h⁻¹, respectively.^[14b] The study of the mecha-

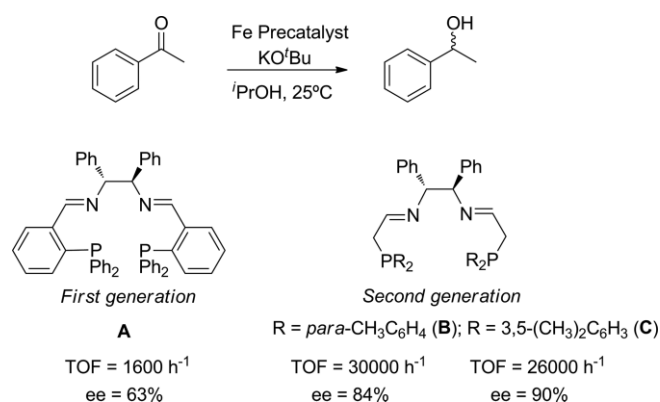
[a] Departament de Química Física i Inorgànica, Universitat Rovira i Virgili, Marcel·li Domingo s/n, 43007, Tarragona, Spain
E-mail: Cyril.godard@urv.cat

[b] Department of Chemical and Pharmaceutical Science, University of Trieste, Via Giorgieri 1, Trieste, Italy

[c] Centre Tecnològic de la Química, Marcel·li Domingo s/n, 43007, Tarragona, Spain

Supporting information and ORCID(s) from the author(s) for this article are available on the WWW under <https://doi.org/10.1002/ejic.201900778>.

nism provided evidence for the reduction of one of the imine groups of the starting PNNP ligand during catalysis, giving a highly active catalyst containing an amido and ene-amido functionalities.^[16] The proposed structure of the amido (ene-amido) catalyst was further supported by reaction with acid providing a coordinated ligand that contained an amine and imine functions.^[16] In view of the excellent results obtained with this set of iron(II) complexes, the group of Morris and co-workers developed a *third generation* of iron(II) catalyst containing an imine and an amine function.^[17a] These new set of catalysts was applied in the asymmetric transfer hydrogenation of ketones and imines with enantioselectivities up to 98%. TOFs as high as 200 s⁻¹ were obtained with these new P–N–NH–P iron(II) systems. It is worth mentioning that the *third generation* of iron(II) catalysts provided greater TOF values than ruthenium- and osmium-based (*R,S*)-Josiphos systems and the ruthenium-based P–NH–NH–P complexes, which provided a TOF of 89 and 92 s⁻¹, respectively.^[18,19] Later, the same group showed in the asymmetric transfer hydrogenation of acetophenone, the enantiomeric excess ranged from 94% (*R*) to 95% (*S*) depending on the nature of PR₂ and whether the precatalyst contained an imine or amine donor.^[17b] It should be pointed out that for all generations, the presence of CO in the precatalyst structure was a prerequisite in order to obtain active catalysts.^[10a]



Scheme 2. Chiral PNNP reported by Morris and co-workers in the ATH of ketones.

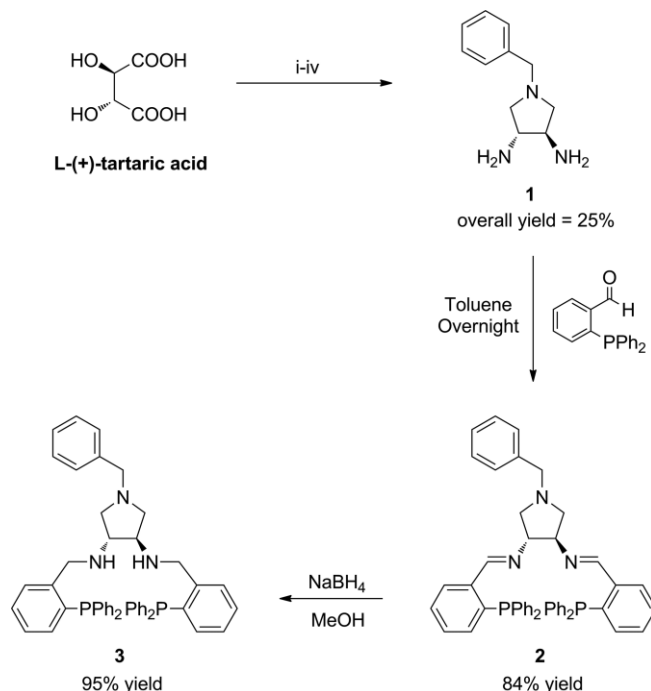
In view of these results, it was thought that the introduction of a pyrrolidine moiety in PNNP ligands could potentially allow the anchoring of the ligand through the functionalization of the NH group. Here, we report a preliminary study including the synthesis of the novel PNNP ligands containing a chiral pyrrolidine backbone, their coordination chemistry with Fe(II) and their application as catalysts in the asymmetric transfer hydrogenation of ketones.

Results and Discussion

Synthesis of the PNNP Ligands **2** and **3**

The chiral PNNP ligand **2** was synthesized by condensation of diamine **1**, which is accessible from L-tartaric acid^[20] in four steps, and the commercially available 2-diphenylphosphino benzaldehyde in 84% yield. Reduction of the diimine with

NaBH₄ in MeOH afforded ligand **3** in quantitative yield (Scheme 3). These new ligands were fully characterized by multinuclear NMR spectroscopy, ESI-HRMS and Elemental Analysis.

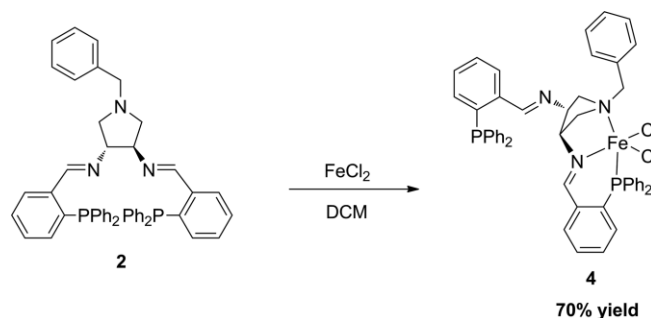


Scheme 3. Synthesis of ligands **2** and **3**. i) Benzylamine, xylene, reflux, 24 h. ii) LiAlH₄, THF, reflux, 48 h. iii) HN₃, PPh₃, DIAD, toluene, r.t., overnight. iv) Pd/C, 1atm H₂, EtOH, overnight.

In the ¹H NMR spectra of ligand **2**, the formation of the ligand was confirmed by the detection of a doublet signal at 8.46 ppm corresponding to the CH=N moiety. In the case of ligand **3**, the disappearance of this signal and the detection of a new signal at 3.84 ppm confirmed the reduction of the imine fragment (CH₂-NH), and thus the formation of ligand **3**. In the ³¹P{¹H} NMR spectrum, a singlet at -12.14 ppm appeared for ligand **2** while that of **3** was observed at -16.21 ppm.

Synthesis of the Bis(chloride) Complex [FeCl₂(**2**)] (**4**)

The pyrrolidine-based PNNP ligand reacts with FeCl₂ in CH₂Cl₂ at room temperature to give the new paramagnetic neutral complex [FeCl₂(**2**)] (**4**) whose formation is indicated by a color change from yellow to pink-red (Scheme 4).



Scheme 4. Synthesis of [FeCl₂(**2**)] (**4**).

The ¹H NMR spectrum showed paramagnetically shifted resonances in the range -30 ppm to 110 ppm. Magnetic measure-

ments (Gouy's method) revealed a magnetic effective moment $\mu_{\text{eff}} = 5.0$. In the $^{31}\text{P}\{^1\text{H}\}$ NMR spectrum at room temperature, a singlet signal was observed at -0.65 ppm, which chemical shift is in the range of the uncoordinated phosphines. For this reason, a low temperature NMR study was performed (Figure 1).

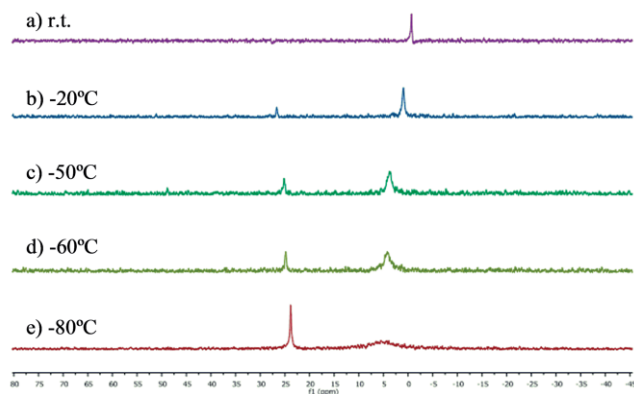
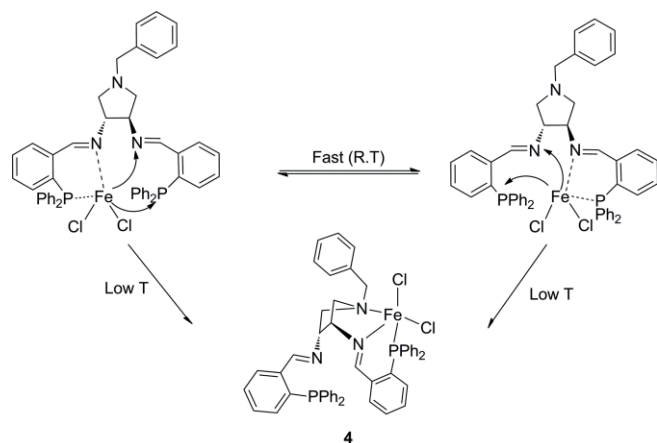


Figure 1. $^{31}\text{P}\{^1\text{H}\}$ NMR spectrum of $[\text{FeCl}_2(\mathbf{2})]$ (**4**) at distinct temperatures. (a) at r.t. (b) at -20°C . (c) at -50°C . (d) at -60°C . (e) at -80°C .

Upon lowering the temperature to -20°C , a new signal was detected at 26.7 ppm (Figure 1b). When the temperature was further lowered from to -80°C (Figure 1c–e), the signal originally detected at -0.65 ppm became broader and was displaced to higher chemical shifts whereas the intensity of the signal at 26.7 ppm became sharper and was displaced to lower chemical shifts. These observations indicated that at room temperature, complex **4** is involved in a fluxional process resulting in the detection of an average signal at -0.65 ppm while at low temperature, only one of the phosphine moieties of the ligand is coordinated to the Fe center.

Crystals suitable for X-ray diffraction were obtained by vapour diffusion from CH_2Cl_2 in pentane at room temperature. The X-ray diffraction analysis revealed the same coordination mode of the ligand to the iron center in the solid state. Figure 2 shows the ORTEP view of complex $[(\text{PNN})\text{FeCl}_2]$ (**4**).

In the solid state the coordination geometry of the iron atom in the chiral PNNP-iron complex **4** is best described as a strongly distorted trigonal bipyramidal (tbp) where N2 and P1 ligand donors occupy the apical positions, while N1 and chlorine atoms are located in the equatorial plane. Deviations from

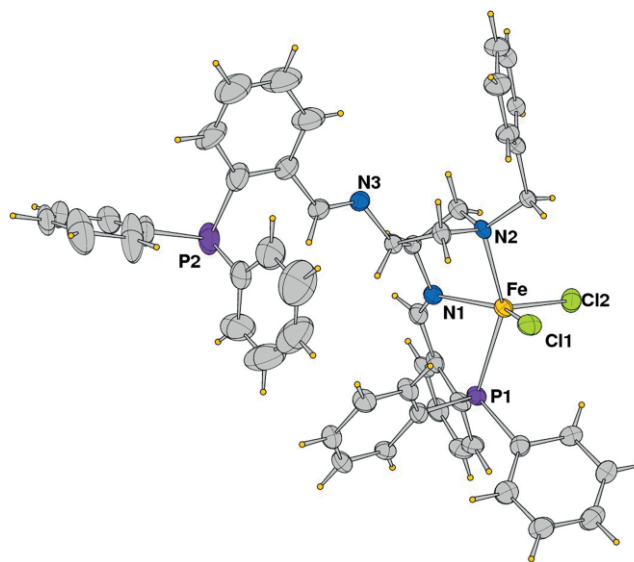


Figure 2. ORTEP drawing of complex $[\text{FeCl}_2(\mathbf{2})]$ (**4**) (ellipsoids at 50 % probability). Solvent molecule omitted for clarity and only partial labeling scheme is illustrated.

the ideal tbp geometry are evidenced in particular by the $\text{N}(2)\text{--Fe--P}(1)$ and $\text{N}(1)\text{--Fe--Cl}(1)$ bond angles of 148.56 and 138.9° , respectively. Similar geometries have been detected in other structurally characterized complexes of type $[(\text{PNN})\text{FeX}_2]$.^[21] The $\text{Fe--N}(1)$ and $\text{Fe--N}(2)$ bond lengths are equivalent [$2.212(5)$ Å], while the Fe--Cl distances are significantly different of $2.3719(17)$ vs. $2.2572(18)$ Å. Finally the $\text{Fe--P}(1)$ bond length of $2.4729(15)$ Å is in agreement with values detected in other previously reported complexes of type $[(\text{PNN})\text{FeCl}_2]$.^[21] Selected bond lengths and distances of complex $[\text{FeCl}_2(\mathbf{2})]$ (**4**) are listed in Table 1.

Table 1. Computed and experimental (Exp) selected bond lengths and non-bonding distances (Å) and angles (deg) for tbp-N1N2 structure of $[\text{FeCl}_2(\mathbf{2}_\text{H})]$ and $[\text{FeCl}_2(\mathbf{2})]$ complexes.

	$\text{FeCl}_2(\mathbf{2}_\text{H})$ d [Å]	$\text{FeCl}_2(\mathbf{2})$ d [Å]	Exp. d [Å]
$\text{Fe--N}(1)$	2.223	2.156	2.212(5)
$\text{Fe--N}(2)$	2.333	2.324	2.212(5)
$\text{Fe--Cl}(1)$	2.359	2.386	2.3719(17)
$\text{Fe--Cl}(2)$	2.361	2.280	2.2572(18)
$\text{Fe--P}(1)$	2.556	2.442	2.4729(15)
$\text{Fe--N}(3)$	4.793	4.834	4.828(1)
$\text{Fe--P}(2)$	7.820	7.874	8.306(1)
	θ [°]	θ [°]	θ [°]
$\text{N}(1)\text{--Fe--N}(2)$	77.5	76.4	75.58(17)
$\text{N}(1)\text{--Fe--Cl}(1)$	130.8	145.2	138.89(15)
$\text{N}(1)\text{--Fe--Cl}(2)$	102.0	100.1	110.86(15)
$\text{N}(2)\text{--Fe--Cl}(1)$	92.9	88.0	92.81(13)
$\text{N}(2)\text{--Fe--Cl}(2)$	96.7	105.0	104.22(9)
$\text{N}(1)\text{--Fe--P}(1)$	82.3	81.0	79.94(13)
$\text{N}(2)\text{--Fe--P}(1)$	157.8	142.7	148.56(11)
$\text{Cl}(1)\text{--Fe--Cl}(2)$	127.1	114.0	110.21(7)

In order to further investigate the stability of related structures for complex **4**, DFT calculations were carried out on the following coordination geometries: (a) a tbp structure (tbp-

N1N2) with one imine and the pyrrolidine nitrogen coordinated to the iron center, (b) a symmetric *tbp* structure (*tbp*-N1N3) with both imines coordinated to the iron center, (c) an octahedral (*oct*-N1N3) and (d) tetrahedral (*td*-N1N3) species (Figure 3). Calculations were carried out using B3LYP functional, dichloromethane as solvent and for each geometry, various multiplicities were considered. To reduce computational cost, the phenyl substituents on phosphorus atoms were first replaced with hydrogen atoms (2_{H}).

In agreement with the experimental results, the most stable structure was the quintuplet ***tbp*-N1N2** complex. Quintuplet ($2S + 1 = 5$) is also the lowest energy state for the other structures. The ***tbp*-N1N3**, ***oct*-N1N3** and ***td*-N1N3** structures fall in a narrow energy range (5–7 kcal mol⁻¹) (Table 2). When the phenyl substituents at the phosphorus atoms were included in the computed structure for the singlet and quintuplet states (Table 1 and Table 2), the quintuplet state of ***tbp*-N1N2** structure remained the most stable isomer while the oct-like (***oct***-

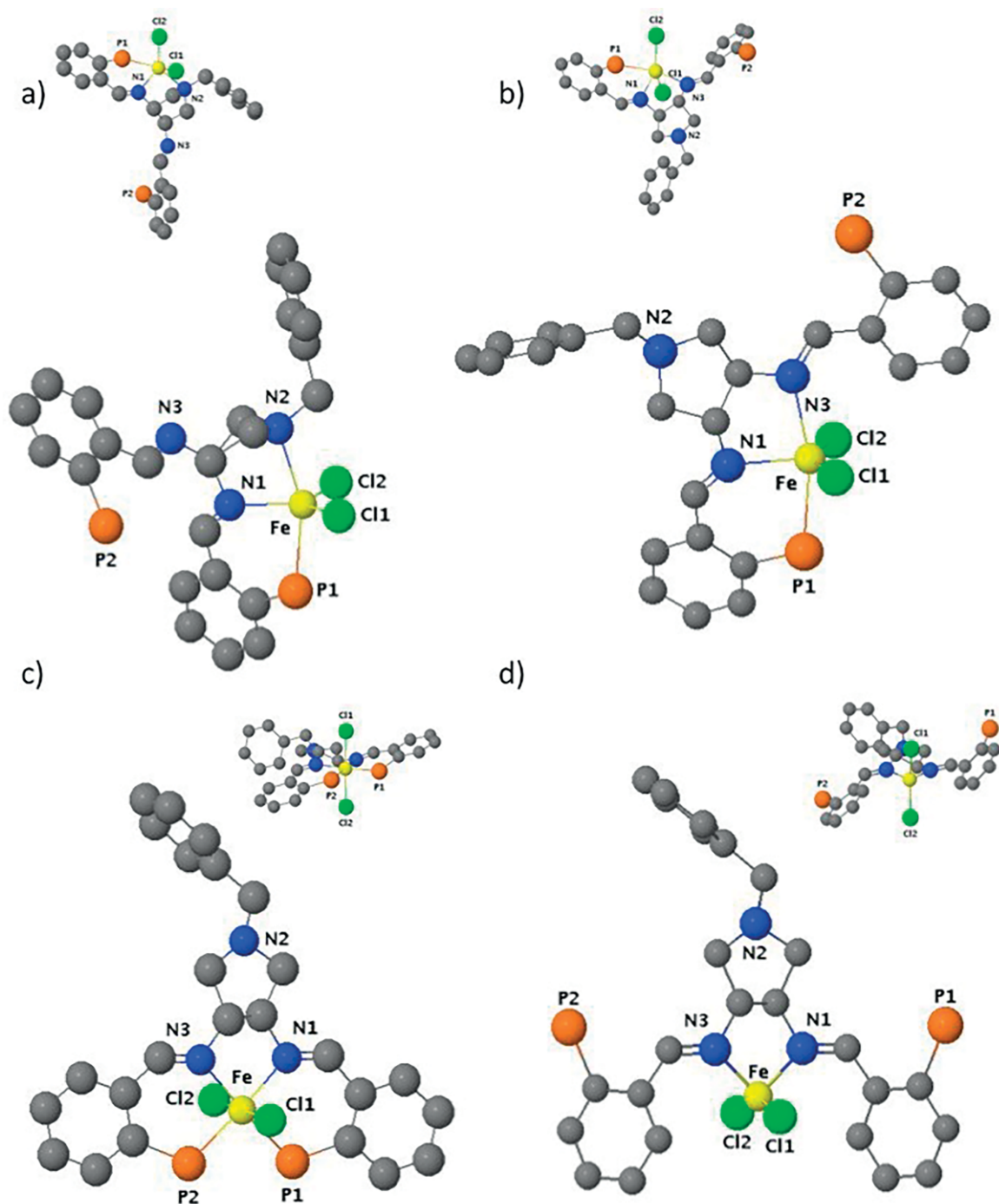


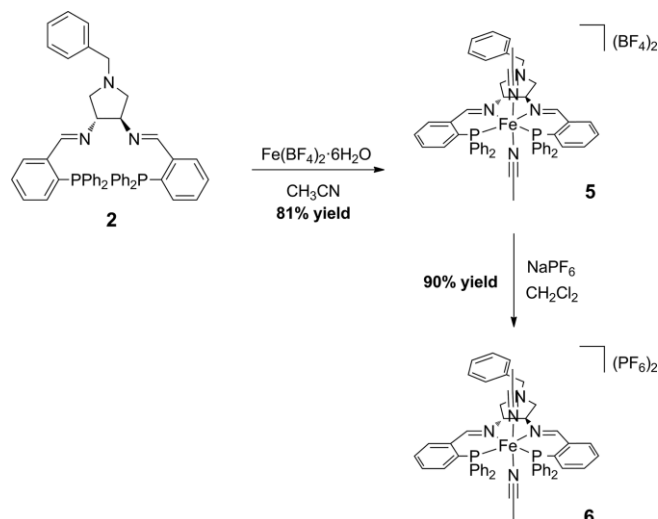
Figure 3. Atom labels for $[\text{FeCl}_2(2_{\text{H}})]$ (a) ***tbp*-N1N2**, (b) ***tbp*-N1N3**, (c) ***oct*-N1N3**, and (d) ***td*-N1N3** structures. Hydrogen atoms are omitted for clarity. Phenyl groups attached to P are not displayed.

N1N3) structure lied 4.7 kcal mol⁻¹ above in energy and in this case, the singlet state was preferred. With these parameters, the energy of the quintuplet state of **tbp-N1N3** structure compared to that of the **tbp-N1N2** increases by 13 kcal mol⁻¹. Interestingly, only a singlet structure very high in energy converged for the td-like structure, indicating that this type of coordination geometry can be discarded.

Table 2. Computed relative energies [kcal mol⁻¹] of complexes [FeCl₂(**2**_H)] and [FeCl₂(**2**)] with different multiplicities (2S + 1).

	2S + 1	tbp-N1N2	oct-N1N3	tbp-N1N3	td-N1N3
[FeCl ₂ (2 _H)]	1	29.7	14.8	33.3	48.1
	3	14.0	19.3	22.8	38.4
	5	0.0	7.1	7.2	5.1
	7	42.5	56.0	53.2	57.0
[FeCl ₂ (2)]	1	19.8	4.7	28.5	44.1
	5	0.0	7.2	13.0	–

Synthesis of the bis(acetonitrile) complexes [Fe(CH₃CN)₂(**2**)](BF₄)₂ (**5**) and [Fe(CH₃CN)₂(**2**)](PF₆)₂ (**6**). The pyrrolidine-base PNNP ligand **2** reacts with Fe(BF₄)₂·6H₂O in CH₃CN to form the diamagnetic dicationic complex **5** (81 % yield) whose formation is indicated by a color change from yellow to orange (Scheme 5). In the presence of NaPF₆, [Fe(CH₃CN)₂(**2**)](BF₄)₂ (**5**) reacts in CH₂Cl₂ at room temperature to provide the diamagnetic dicationic complex [Fe(CH₃CN)₂(**2**)](PF₆)₂ (**6**) in 90 % yield (Scheme 5). The ³¹P{¹H} NMR spectra of both complexes contained two mutually coupled doublet signals at ca. 51 and 52 (²J_{p-p'} = 42–44 Hz), indicating the presence of two slightly inequivalent phosphine moieties in the complex. These chemical shifts were similar to those observed by Morris and co-workers for the iron(II) PNNP complexes [Fe(MeCN)₂(A)](BF₄)₂ (51.8), although in that case, a singlet signal was reported.^[10c]



Scheme 5. Formation of [Fe(CH₃CN)₂(**2**)](BF₄)₂ (**5**) and [Fe(CH₃CN)₂(**2**)](PF₆)₂ (**6**).

Crystals suitable for X-ray diffraction were obtained by vapour diffusion of pentane into a CH₂Cl₂ solution containing complex **6**. To our surprise, the X-ray structural analysis revealed a Fe(III) complex, [Fe(CH₃CN)₂(**2**)](PF₆)₃, where the ligand **2** is coordinated to the iron center in a tetradentate manner. This fact is tentatively

attributed to an oxidation of the Fe during the course of the crystallization since no sign of paramagnetism was observed in the NMR spectra of the complex **6**. The molecular structure of this complex is displayed in Figure 4, while the coordination bond lengths and angles are reported in Table 3.

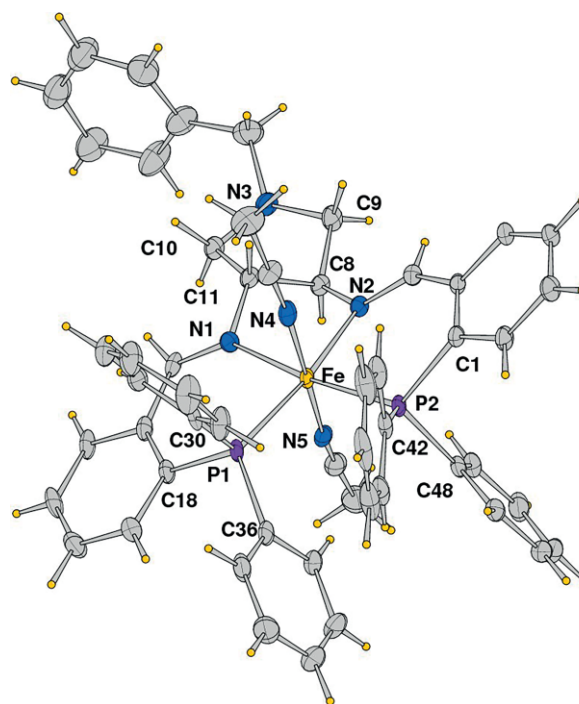


Figure 4. ORTEP drawing of the complex [Fe(CH₃CN)₂(**2**)](PF₆)₃ (ellipsoid probability at 50 %). Solvent molecules and anions are omitted and only a partial labeling scheme is shown for clarity.

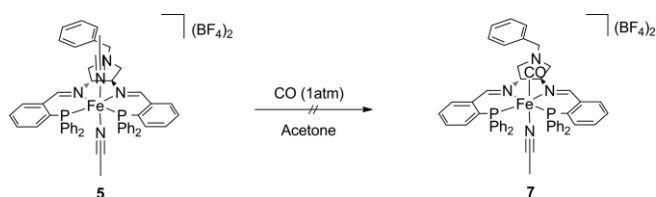
Table 3. Selected bond lengths [Å] and angles [deg] for complex [Fe(CH₃CN)₂(**2**)](PF₆)₃.

Bond lengths			
Fe–N(1)	2.042(4)	Fe–N(5)	1.923(5)
Fe–N(2)	2.039(4)	Fe–P(1)	2.2573(14)
Fe–N(4)	1.905(6)	Fe–P(2)	2.2800(13)
Bond angles			
N(1)–Fe–N(2)	83.96(17)	N(1)–Fe–P(2)	172.88(14)
N(4)–Fe–N(5)	173.3(2)	N(2)–Fe–P(1)	172.32(12)
P(1)–Fe–P(2)	97.51(5)	N(2)–Fe–P(2)	89.76(11)
N(1)–Fe–N(4)	87.9(2)	N(4)–Fe–P(1)	91.12(16)
N(1)–Fe–N(5)	86.5(2)	N(4)–Fe–P(2)	88.35(14)
N(2)–Fe–N(4)	86.6(2)	N(5)–Fe–P(1)	92.52(16)
N(2)–Fe–N(5)	89.1(2)	N(5)–Fe–P(2)	96.73(15)
N(1)–Fe–P(1)	88.63(13)		

In this complex, the iron center exhibits a distorted octahedral geometry where equatorial positions are occupied by the P₂N₂ donor set of the ligand **2** and linearly coordinated CH₃CN molecules are at axial positions. The Fe–N(imine) bond lengths are comparable within their esd's [2.042(4) and 2.039(4) Å], as well as the Fe–NCCH₃ distances, of 1.905(6) and 1.923(5) Å. On the other hand, the values of the Fe–P bond lengths are significantly different [2.2573(14) and 2.2800(13) Å]. This Fe(III) complex crystallizes with a disordered lattice molecule of pentane beside the PF₆ anions.

Attempted Synthesis of the Acetonitrilecarbonyl Complex [Fe(CH₃CN)(CO)(2)](BF₄)₂ (**7**)

The reaction was carried out using the standard procedure described for this transformation.^[10a] The complex [Fe(CH₃CN)₂(**2**)](BF₄)₂ (**5**) was reacted in acetone under CO atmosphere (1atm) at room temperature for 16 h. However, the resulting ³¹P{¹H} NMR spectrum only revealed the presence of the starting ligand **2**. Various strategies were tested to obtain complex **7**, however, all attempts proved unsuccessful (Scheme 6).



Scheme 6. Attempted synthesis of complex [Fe(CH₃CN)(CO)(2)](BF₄)₂ (**7**).

We performed DFT calculations, using B3LYP functional and acetone as solvent, for different structures and multiplicities of the complexes [Fe(CH₃CN)₂(**2**)]²⁺ and [Fe(CH₃CN)(CO)(**2**)]²⁺. The most stable structure is the low spin (singlet) oct structure for both complexes, in agreement with experimental results for bis(acetonitrile) complex. The quintuplet-tbpN1N2 structure only lies 5.8 kcal mol⁻¹ higher in energy for [Fe(CH₃CN)₂(**2**)]²⁺ but is 20.0 kcal mol⁻¹ higher in the case of [Fe(CH₃CN)₂(CO)(**2**)]²⁺.

Other computed structures of [Fe(CH₃CN)₂(**2**)]²⁺ calculated were between 9 and 19 kcal mol⁻¹ higher in energy than the singlet oct structure (see supporting information for details).

Finally, the computed free energy for the substitution reaction (Scheme 4) is of -3.2 kcal mol⁻¹. Consequently, from a thermodynamic point of view, [Fe(CH₃CN)(CO)(**2**)]²⁺ could be obtained. It was therefore concluded that the impossibility to obtain this complex from **5** must arise from kinetic issues. Unraveling kinetic aspects is out of the scope of the present work.

Asymmetric transfer hydrogenation (ATH) of ketones. The bis(acetonitrile) complexes [Fe(CH₃CN)₂(**2**)](BF₄)₂ (**5**) and [Fe(CH₃CN)₂(**2**)](PF₆)₂ (**6**) were tested as catalyst precursors in the asymmetric transfer hydrogenation of ketones in isopropanol. However, both complexes were inactive in this transformation, in agreement with the reports by Morris and co-workers.^[14a] These authors indeed reported that a carbonyl ligand is necessary to make these types of iron complexes active.

The use of in situ catalytic systems using the PNNP ligand **2** with various iron precursors was therefore investigated for the asymmetric transfer hydrogenation of isobutyrophenone (Table 4). As expected, using Fe(BF₄)₂·6H₂O (entry 1) as precursor, no conversion was observed. However, the use of the iron carbonyl cluster Fe₃(CO)₁₂ as metal source achieved high conversion and excellent enantioselectivity for this transformation (entry 2). It is important to note that for blank experiments, namely in the absence of ligand (entry 3) or of iron source (entry 4), no reaction was observed. When the iron hydride carbonyl cluster complex [Et₃NH][HFe₃(CO)₁₁] was tested, isobutyrophenone was transformed with 98 % conversion and 97 % ee (entry 5). This feature might suggest that a similar active catalyst is formed when the iron carbonyl cluster Fe₃(CO)₁₂ or the iron hydride carbonyl clus-

ter [Et₃NH][HFe₃(CO)₁₁] are used. In view of the results obtained with the iron carbonyl clusters, other iron(0) carbonyl precursors were tested (entries 6 and 7). Nevertheless, when Fe₂(CO)₉ or Fe(CO)₅ were used, no conversion was obtained. When Fe(CO)₅ was used with a ligand/Fe ratio of 1:3 (entry 8) or a combination of Fe(CO)₅/Fe₂(CO)₉ (1:1) (entry 9), no relevant conversion was achieved either. It should be mentioned that Gao and co-workers reported similar observation in the asymmetric transfer hydrogenation of ketones catalyzed by PNNHP ligands.^[22]

Table 4. Asymmetric transfer hydrogenation of isobutyrophenone catalyzed by Fe/**2**. Screening of iron precursors.^[a]

Entry	Iron precursor	Conv. [%] ^[b]	ee [%] ^[b]
1	Fe(BF ₄) ₂ ·6H ₂ O	0	–
2	Fe ₃ (CO) ₁₂	97	96
3	Fe ₃ (CO) ₁₂ ^[c]	0	–
4	–	0	–
5	[Et ₃ NH][HFe ₃ (CO) ₁₁]	98	97
6	Fe ₂ (CO) ₉	< 5	85
7	Fe(CO) ₅ ^[d]	0	–
8	Fe(CO) ₅ ^[e]	8	50
9	Fe ₂ (CO) ₉ /Fe(CO) ₅	< 5	10

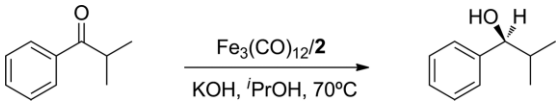
[a] General conditions: Fe/**2**/KOH = 1:1:8; 0.0068 mmol of Fe, 0.0068 mmol of **2**, 0.054 mmol of KOH, 0.136 mmol of isobutyrophenone, 3 mL of *i*PrOH, time = 16 h, temperature = 70 °C. [b] Conversion and enantiomeric excess was calculated by GC using a ChirasilDex CB column. [c] No ligand used. [d] Ligand/Fe = 1:1. [e] Ligand/Fe = 1:3.

The nature and the amount of base in the catalytic reaction using the iron carbonyl cluster Fe₃(CO)₁₂ as iron source were examined (Table 5). The best results were obtained when KOH was used as base, with 97 % conversion and 96 % of enantioselectivity (entry 1). The use of NaOH considerably lowered the conversion whereas the enantioselectivity was maintained (entry 2). When the basicity was increased, lower conversions were also observed although the enantiomeric ratio remained high (entry 3). However, when NaO*i*Pr was used, no activity was observed (entry 4). Decreasing the amount of KOH from a ratio of 1:8 to 1:1 had a strong impact on the activity while the enantioselectivity slightly decreased (entry 7–9).

The effect of the temperature and catalyst loading was also examined obtaining an optimal temperature of 70 °C and 5 mol-% of catalyst loading (see supporting information for details).

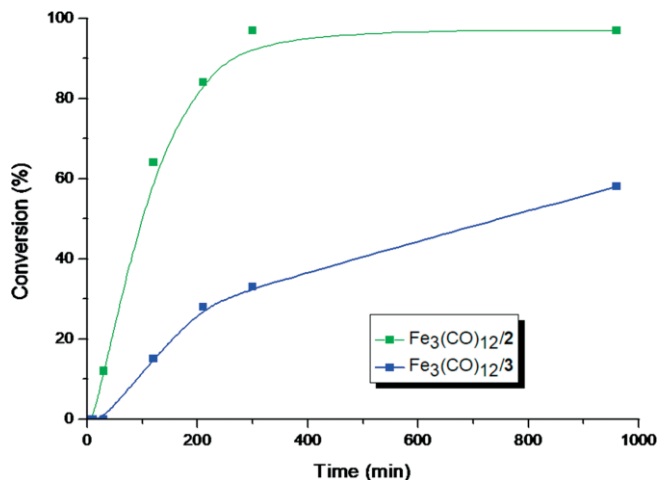
Monitoring of the performance of the catalytic systems containing the PNNP ligands **2** and **3** using 5 mol-% of catalyst loading, Fe₃(CO)₁₂ as iron source, at 70 °C of temperature and 16 h of reaction time is depicted in Scheme 7. It should be pointed out that both systems exhibited similar enantioselectivities (≈ 97 %) while displayed very distinct activities. Comparing the initial turnover frequencies (TOF h⁻¹) of both systems at ca. 15 % of conversion, the Fe₃(CO)₁₂/**2** catalytic system is three times more active (TOF: 4.8 h⁻¹) than its diamino analogue {Fe₃(CO)₁₂/**3**} (TOF: 1.5 h⁻¹). After 500 minutes, the Fe₃(CO)₁₂/**2** system provided a conversion of 95 % whereas the Fe₃(CO)₁₂/**3** system only exhibited ca. 40 % conversion.

Table 5. Asymmetric transfer hydrogenation of isobutyrophenone catalyzed by $\text{Fe}_3(\text{CO})_{12}/\mathbf{2}$. Optimization of the base.^[a]



Entry	Base	L/Base	Conv. [%] ^[b]	ee [%] ^[b]
1	KOH	1:8	97	96
2	NaOH	1:8	46	91
3	KOtBu	1:8	70	86
4	NaO/iPr	1:8	0	–
5	–	–	0	0
6	KOH	1:10	98	97
7	KOH	1:4	38	89
8	KOH	1:2	32	86
9	KOH	1:1	25	83

[a] General conditions: $\text{Fe}_3(\text{CO})_{12}/\mathbf{2}/\text{KOH} = 1:1:8$; 0.0068 mmol of $\text{Fe}_3(\text{CO})_{12}$, 0.0068 mmol of $\mathbf{2}$, 0.054 mmol of KOH, 0.136 mmol of isobutyrophenone, 3 mL of *i*PrOH, time = 16 h, temperature = 70 °C. [b] Conversion and enantiomeric excess was calculated by GC using a ChirasilDex CB column.



Scheme 7. Catalytic performance of $\text{Fe}_3(\text{CO})_{12}/\mathbf{2}$ vs. $\text{Fe}_3(\text{CO})_{12}/\mathbf{3}$.

Asymmetric Transfer Hydrogenation (ATH) of Ketones: Substrate Scope

Based on the reaction conditions, the scope and limitation of the $\text{Fe}_3(\text{CO})_{12}/\mathbf{2}$ catalytic system were explored in the asymmetric transfer hydrogenation of a variety of ketones. The results are summarized in Figure 5.

The hydrogenation of acetophenone provided high conversion towards the corresponding alcohol together with a modest enantioselectivity (35 % ee). Upon increasing the steric bulk at the aliphatic position of the ketone, an increase of the enantiomeric excess was observed (Me < Et < *i*Pr = *t*Bu) with enantioselectivities up to 96 % in the case of isobutyrophenone. Following the same trend, isovalerophenone exhibited high conversion (94 %) and enantioselectivities in a range between isobutyrophenone and *tert*-butyl phenyl ketone (73 % ee). It has to be mentioned that replacing the phenyl group of the acetophenone by the naphthalene ring gave similar results in terms of conversion as well as enantiomeric excess. Then, the reduction of cyclic

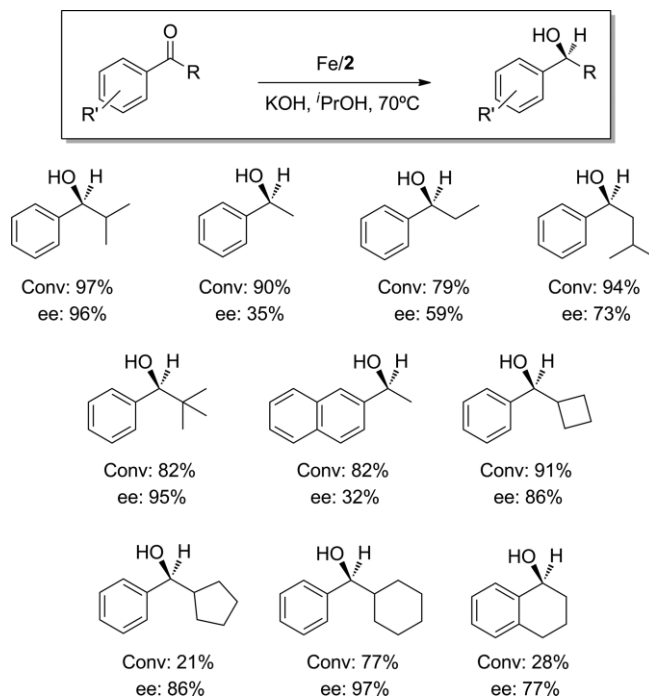


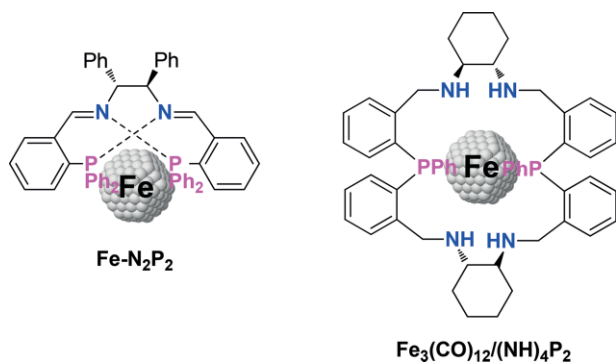
Figure 5. Scope and limitations of the asymmetric transfer hydrogenation of a variety of ketones catalyzed by the $\text{Fe}_3(\text{CO})_{12}/\mathbf{2}$ system. General conditions: $\text{Fe}_3(\text{CO})_{12}/\mathbf{2}/\text{KOH} = 1:1:8$; 0.0068 mmol of $\text{Fe}_3(\text{CO})_{12}$, 0.0068 mmol of $\mathbf{2}$, 0.054 mmol of KOH, 0.136 mmol of Ketone, 3 mL of *i*PrOH, time = 16 h, temperature = 70 °C. Conversion and enantiomeric excess were calculated by GC using a ChirasilDex CB column.

phenyl ketones and ketones containing annulated-rings was carried out. The reduction of cyclobutyl phenyl ketone provided high conversion and enantioselectivities. However, when more flexible rings were located in the α -position of the ketone, such as cyclopentyl and cyclohexyl phenyl ketone, lower conversions were observed although the ee's remained unchanged or even increased in the case of cyclohexyl phenyl ketone up to 97 %. Finally, when the 3,4-dihydronaphthalen-1(2*H*)-one was employed as substrate, low conversion was obtained and the enantioselection was moderate.

Mechanistic Observations

Previous studies conducted by the groups of Morris^[15,23] and Gao^[24] with similar Fe-N₂P₂ and $\text{Fe}_3(\text{CO})_{12}/(\text{NH})_4\text{P}_2$ (Scheme 8) catalytic systems, have proven to be heterogeneous rather than homogeneous, involving iron nanoparticles as the active catalytic species. Various poisoning agents such as phosphines, sulfides, or mercury have been used in order to differentiate an homogeneous process from a heterogeneous one.^[25] In this regard, we have chosen Hg(0) to carry out the poisoning experiment, a poison usually used to distinguish homogeneous catalysis from catalysis by metal particles.

First of all, the reaction mixture is cloudy throughout the entire ATH process, as previously seen by other groups.^[24] In our case, the use of 3eq of Hg was sufficient to stop the ATH completely. This result is in agreement with the previous work reported by Gao and co-workers with similar in situ systems.^[24]



Scheme 8. Previous heterogeneous $\text{Fe-N}_2\text{P}_2$ and $\text{Fe}_3(\text{CO})_{12}/(\text{NH})_4\text{P}_2$ catalytic systems reported for the ATH and AH of ketones respectively.

Consequently, it is suggested that the ATH catalyzed by $\text{Fe}_3(\text{CO})_{12}/\mathbf{2}$ is probably heterogeneous, having $\mathbf{2}$ -modified iron particles acting as active catalyst.

Conclusions

The novel PNNP ligands $\mathbf{2}$ and $\mathbf{3}$ containing a pyrrolidine scaffold have been synthesized and fully characterized by NMR, ESI-HRMS and EA. The incorporation of the pyrrolidine backbone could potentially allow the anchoring of the ligand through the functionalization of the NH group. The reaction between ligand $\mathbf{2}$ and iron(II) precursors enables the synthesis of monomeric complexes stable and paramagnetic in the case of complex $[\text{FeCl}_2(\mathbf{2})]$ ($\mathbf{4}$) or diamagnetic in the case of $[\text{Fe}(\text{CH}_3\text{CN})_2(\mathbf{2})]$ ($\mathbf{5}$) and $[\text{Fe}(\text{CH}_3\text{CN})_2(\mathbf{2})]$ (PF_6) ($\mathbf{6}$). The obtained iron(II) complexes were characterized by NMR, ESI-HRMS, EA and by X-ray diffraction for $\mathbf{4}$ and $\mathbf{6}$. DFT calculations were carried out for complex $[\text{FeCl}_2(\mathbf{2})]$ ($\mathbf{4}$) in order to investigate the stability of different coordination isomers, obtaining the quintuplet tbp-N1N2 as the most stable complex. Similarly, theoretical computation for $[\text{Fe}(\text{CH}_3\text{CN})_2(\mathbf{2})]$ (BF_4) ($\mathbf{5}$) indicated the low spin (singlet) oct-N1N3 complex as the most stable species. The impossibility to obtain complex $[\text{Fe}(\text{CH}_3\text{CN})(\text{CO})(\mathbf{2})]$ (BF_4) ($\mathbf{7}$) was attributed to kinetic arguments. The PNNP ligands $\mathbf{2}$ and $\mathbf{3}$ were used in combination with $\text{Fe}_3(\text{CO})_{12}$ in the asymmetric transfer hydrogenation of a variety of ketones and provided low to high conversions (21–97 %) and enantioselectivities (32–97 %) depending of the substrate. Upon increasing the steric bulk at the aliphatic position of the ketone, higher enantioselectivities were achieved, up to 97 % when isobutyrophenone was used as substrate. From a mechanistic point of view, it is suggested that the $\text{Fe}_3(\text{CO})_{12}/\mathbf{2}$ system is probably heterogeneous, in nature. The introduction of the pyrrolidine thus did not affect substantially the asymmetric induction, when compared with the results previously reported using related ligands.

Experimental Section

General Considerations: All preparations and manipulations were carried out under an oxygen-free nitrogen atmosphere using conventional Schlenk techniques or inside a glovebox. Solvents were purified by the system Braun MB SPS-800 and stored under nitrogen

atmosphere. CH_3CN , $i\text{PrOH}$ and MeOH were dried, distilled and degassed using standard procedure.^[26] Deuterated solvents were degassed via three freeze-pump-thaw cycles and kept in the glovebox over 4 Å molecular sieves. Reagents were purchased from Aldrich, Alfa Aesar and Strem. ^1H , ^{13}C , ^{31}P , ^{11}B and ^{19}F NMR spectra were recorded on a Varian Mercury VX 400 (400 MHz, 100.6 MHz, 162 MHz, 128.5 MHz and 376.8 MHz respectively). Chemical shift values for ^1H and ^{13}C were referred to internal SiMe_4 (0.0 ppm) and for ^{31}P was referred to H_3PO_4 (85 % solution in D_2O , 0 ppm). 2D correlation spectra (gCOSY, gHSQC and gHMBC) were visualized using VNMR program (Varian®). Enantiomeric ratios were determined by GC analysis. Gas chromatography analyses were carried out in a Hewlett-Packard HP 6890 gas chromatograph, using the CP Chirasil-Dex CB chiral column. ESI-HMRS and EA were performed at the Serveis Tècnics de Recerca from the Universitat de Girona (Spain).

Synthesis of (2): 2-(diphenylphosphino)benzaldehyde (0.155g, 0.53 mmol) was added to 4 mL of dry and degassed toluene provided with molecular sieves. Then, (3R,4R)-3,4-diamino-1-benzylpyrrolidine ($\mathbf{1}$) (49.7 mg, 0.26 mmol) was added to the mixture. This solution was allowed to stir overnight at 90 °C. The reaction mixture was filtered under nitrogen atmosphere and collected by vacuum filtration. Recrystallization with cool MeOH in a glovebox afforded a yellow solid in 84 % yield. $^1\text{H-NMR}$ (CD_2Cl_2 , 400 MHz, δ in ppm): 8.45 (d, 2H, $J = 4\text{Hz}$, HC=N), 7.80 (m, 2H, Ar-), 7.38 (m, 2H, Ar-), 7.33 (d, 4H, $J = 8\text{Hz}$, Ar-), 7.29–7.18 (m, 23H, Ar-), 6.85 (m, 2H, Ar-), 3.59 (d, 1H, $J = 4\text{Hz}$, $-\text{CH}_2\text{-Ph}$, $-\text{CH}_2\text{-}$), 3.55 (d, 1H, $J = 4\text{Hz}$, $-\text{CH}_2\text{-Ph}$, $-\text{CH}_2\text{-}$), 3.48 (quint, 2H, $J = 4\text{Hz}$, $-\text{CH-}$), 2.70 (dd, 2H, $J = 4 \& 8\text{Hz}$, $-\text{CH}_2\text{-}$), 2.46 (dd, 2H, $J = 4 \& 8\text{Hz}$, $-\text{CH}_2\text{-}$). $^{13}\text{C}\{^1\text{H}\}\text{-NMR}$ (CD_2Cl_2 , 100.6 MHz, δ in ppm): 159.4 (d, $J_{\text{C-P}} = 16\text{Hz}$, HC=N), 134.2, 134.0, 133.8, 133.5, 129.9, 128.8, 128.7, 128.5, 128.4, 128.3, 128.1, 126.8, overlapped signals, 75.8 ($-\text{CH-}$), 60.4 ($-\text{CH}_2\text{-}$), 60.2 ($-\text{CH}_2\text{Ph}$). $^{31}\text{P}\{^1\text{H}\}\text{-NMR}$ (CD_2Cl_2 , 161MHz, δ in ppm): -12.14 . ESI-HRMS: Calculated for $\text{C}_{49}\text{H}_{43}\text{N}_3\text{P}_2$: Exact: (M: 735.29; [M + H] $^+$: 736.29); Experimental ([M + H] $^+$: 736.2997). Elemental Analysis: Calculated for $\text{C}_{49}\text{H}_{43}\text{N}_3\text{P}_2$: C, 79.98; H, 5.89; N, 5.71; found C, 79.09; H, 5.73; N, 5.37.

Synthesis of (3): ($\mathbf{2}$) (90 mg, 0.12 mmol) was dissolved in 5 mL of dry methanol. Then, NaBH_4 (28 mg, 0.73 mmol) was added under nitrogen atmosphere. The reaction was refluxed with stirring under nitrogen for 24 h. The solution was cooled to room temperature and deoxygenated H_2O (3 mL) was added to destroy the excess of NaBH_4 . The mixture solution was extracted with deoxygenated CH_2Cl_2 (3 mL \times 3). The organic layer was dried with anhydrous MgSO_4 and evaporation under vacuum afforded the product in 95 % yield. $^1\text{H-NMR}$ (CD_2Cl_2 , 400 MHz, δ in ppm): 7.45–7.42 (m, 3H, Ar-), 7.32–7.19 (m, 26H, Ar-), 7.16–7.12 (m, 2H, Ar-), 6.87–6.84 (m, 2H, Ar-), 3.84 (qd, 4H, $J = 12 \& 4\text{Hz}$, $\text{CH}_2\text{-NH}$, $-\text{CH}_2\text{-}$), 3.43 (s, 2H, $-\text{CH}_2\text{-Ph}$, $-\text{CH}_2\text{-}$), 2.80 (quint, 2H, $J = 4\text{Hz}$, $-\text{CH-}$), 2.55 (dd, 2H, $J = 4 \& 12\text{Hz}$, $-\text{CH}_2\text{-}$), 2.11 (dd, 2H, $J = 4 \& 12\text{Hz}$, $-\text{CH}_2\text{-}$). $^{13}\text{C}\{^1\text{H}\}\text{-NMR}$ (CD_2Cl_2 , 100.6 MHz, δ in ppm): 145.0 (d, $^2J_{\text{C-P}} = 24.1\text{Hz}$, Ar-, $-\text{C-}$), 139.4 (CH_2Ph , Ar-, $-\text{C-}$), 137.2 (d, $^1J_{\text{C-P}} = 11.1\text{Hz}$, PPh_2 , Ar-, $-\text{C-}$), 137.1 (d, $^1J_{\text{C-P}} = 11.1\text{Hz}$, PPh_2 , Ar-, $-\text{C-}$), 135.9 (d, $^1J_{\text{C-P}} = 11.1\text{Hz}$, Ar-, $-\text{C-}$), 133.9 (d, $J = 2\text{Hz}$, Ar-, $-\text{CH-}$), 133.8 (d, $J = 2\text{Hz}$, Ar-, $-\text{CH-}$), 133.5 (Ar-, $-\text{CH-}$), 129.3 (d, $J = 5\text{Hz}$, Ar-, $-\text{CH-}$), 128.9 (Ar-, $-\text{CH-}$), 128.8 (Ar-, $-\text{CH-}$), 128.7 (d, $J = 3\text{Hz}$, Ar-, $-\text{CH-}$), 128.6 (d, $J = 3\text{Hz}$, Ar-, $-\text{CH-}$), 128.5 (d, $J = 3\text{Hz}$, Ar-, $-\text{CH-}$), 128.1 (Ar-, $-\text{CH-}$), 127.1 (Ar-, $-\text{CH-}$), 126.7 (Ar-, $-\text{CH-}$), overlapped signals, 64.3 (CH-NH , $-\text{CH-}$), 60.2 ($\text{CH}_2\text{-Ph}$, $-\text{CH}_2\text{-}$), 59.7 ($\text{CH}_2\text{-CH-NH}$, $-\text{CH}_2\text{-}$), 50.8 (d, $^3J_{\text{C-P}} = 21.1\text{Hz}$, $\text{CH}_2\text{-NH}$, $-\text{CH}_2\text{-}$). $^{31}\text{P}\{^1\text{H}\}\text{-NMR}$ (CD_2Cl_2 , 161MHz, δ in ppm): -16.21 . ESI-HRMS: Calculated for $\text{C}_{49}\text{H}_{45}\text{N}_3\text{P}_2$: Exact: (M: 739.32; [M + H] $^+$: 740.32); Experimental ([M + H] $^+$: 740.37).

Synthesis of $[\text{Fe}(\text{Cl})_2(\mathbf{2})]$ ($\mathbf{4}$): Iron dichloride anhydrous (12 mg, excess) dissolved in 1 mL of CH_2Cl_2 was added to a solution of (*R,R*)- $\{\text{PPh}_2(2\text{-C}_6\text{H}_4)\text{CH}=\text{N}(\text{pyrrolidine-NBn})\}_2$ ($\mathbf{2}$) (50 mg, 0.068 mmol) in

3 mL of CH_2Cl_2 . The mixture was allowed to stir at room temperature for 48 h to which a change of color was appreciated from pale yellow to pink-red. The mixture was filtered via cannula under nitrogen atmosphere and ether was added to the pink-red solution to force the product precipitation. The product was isolated as a pink-red solid in 70 % of yield. Crystals suitable for X-ray diffraction were ground by vapor diffusion of pentane into CH_2Cl_2 solution of the complex. $^1\text{H-NMR}$ (CD_2Cl_2 , 400 MHz, δ in ppm): 105.08, 85.55, 72.60, 60.50, 16.48, 15.43, 12.66, 10.33, 9.94, 8.04, 7.56, 7.32, 7.22, 6.87, 6.72, 6.54, 6.17, 6.02, -1.01, -7.17, -30.37. $^{31}\text{P}\{^1\text{H}\}$ -NMR at r.t. (CD_2Cl_2 , 161MHz, δ in ppm): -0.694. $^{31}\text{P}\{^1\text{H}\}$ -NMR at -80 °C (CD_2Cl_2 , 161MHz, δ in ppm): 23.83 & 5.32 (bs). ESI-HRMS: Calculated for $\text{C}_{49}\text{H}_{43}\text{FeN}_3\text{P}_2\text{Cl}_2$: Exact: (M: 861.1659, M - Cl: 826.1970); Experimental (M - Cl: 826.1986). Elemental Analysis: Calculated for $\text{C}_{49}\text{H}_{43}\text{FeN}_3\text{P}_2\text{Cl}_2 \cdot 0.5\text{CH}_2\text{Cl}_2$: C, 65.69; H, 4.90; N, 4.64; found C, 65.89; H, 4.66; N, 4.16.

Synthesis of $[\text{Fe}(\text{MeCN})_2(\mathbf{2})](\text{BF}_4)_2$ (5**):** (**2**) (0.135 mmol) in 4 mL of MeCN was added to a solution of $\text{Fe}(\text{BF}_4)_2 \cdot 6\text{H}_2\text{O}$ (0.133 mmol) in 1 mL of MeCN. After stirring for 3 h, the red solution was evaporated to dryness. Then, 1 mL of CH_2Cl_2 was added to re-dissolve the deep red powder. Ether (8 mL) was added to the solution and a precipitate started to form. The solid was filtered under nitrogen via cannula and washed repeatedly with ether to afford an orange solid in 81 % yield. $^1\text{H-NMR}$ (CD_2Cl_2 , 400 MHz, δ in ppm): 8.82–8.77 (m, 2H, CH=CN), 8.06–7.96 (m, 3H, Ar-), 7.77–7.21 (m, 21H, Ar-), 6.99 (t, 1H, $J = 8\text{Hz}$, Ar-), 6.88 (t, 1H, $J = 8\text{Hz}$, Ar-), 6.79–6.68 (m, 5H, Ar-), 6.43 (t, 2H, $J = 8\text{Hz}$ Ar-), 5.32 (s, 2H, $\text{CH}_2\text{-Ph}$, $-\text{CH}_2-$), 4.98–4.92 (m, 1H, $-\text{CH}-$), 4.80–4.71 (m, 2H, $-\text{CH}_2-$), 4.55–4.50 (m, 1H, $-\text{CH}_2-$), 4.19–4.07 (m, 2H, $-\text{CH}_2-$), 1.87 (s, 3H, CH_3CN , $-\text{CH}_3$), 1.76 (s, 3H, CH_3CN , $-\text{CH}_3$). $^{31}\text{P}\{^1\text{H}\}$ -NMR (CD_2Cl_2 , 161MHz, δ in ppm): 52.32 (d, $J_{\text{P-P}} = 42\text{Hz}$) and 51.65 ($J_{\text{P-P}} = 42\text{Hz}$). $^{11}\text{B}\{^1\text{H}\}$ -NMR (CD_2Cl_2 , 128.51MHz, δ in ppm): -1.03. $^{19}\text{F}\{^1\text{H}\}$ -NMR (CD_2Cl_2 , 376.8MHz, δ in ppm): -150.05. ESI-HRMS: Calculated for $\text{C}_{53}\text{H}_{49}\text{B}_2\text{F}_8\text{FeN}_5\text{P}_2$: Exact: [M: 1047.2871, M - (CH_3CN) $_2(\text{BF}_4)_2$ /Z: 395.6136]; Experimental [M - (CH_3CN) $_2(\text{BF}_4)_2$ /Z: 395.6146]. Elemental Analysis: Calculated for $\text{C}_{53}\text{H}_{49}\text{B}_2\text{F}_8\text{FeN}_5\text{P}_2 \cdot 3\text{CH}_2\text{Cl}_2$: C, 51.65; H, 4.26; N, 5.38; found C, 51.62; H, 4.49; N, 5.61.

Synthesis of $[\text{Fe}(\text{MeCN})_2(\mathbf{2})](\text{PF}_6)_2$ (6**):** NaPF_6 (16 mg, 0.095 mmol) was added to a solution of **5** (50 mg, 0.047 mmol) in dichloromethane (4 mL). After stirring for 1 h the resulting orange mixture was filtered through a small pad of Celite and the solvents evaporated to dryness to give **6** as an orange solid in 90 % yield. $^1\text{H-NMR}$ (CD_2Cl_2 , 400 MHz, δ in ppm): 8.80 (br s, 1H, CH=CN), 8.71 (br s, 1H, CH=CN), 8.04–7.97 (m, 2H, Ar-), 7.78–7.20 (m, 22H, Ar-), 7.02 (t, 1H, $J = 8\text{Hz}$, Ar-), 6.87 (t, 1H, $J = 8\text{Hz}$, Ar-), 6.80–6.71 (m, 5H, Ar-), 6.36 (t, 2H, $J = 8\text{Hz}$, Ar-), 5.21–5.14 (m, 1H, $-\text{CH}-$), 4.82–4.76 (m, 4H, $-\text{CH}_2-$), 4.55–4.50 (m, 1H, $-\text{CH}-$), 4.13–4.08 (m, 2H, $-\text{CH}_2-$), 1.86 (s, 3H, CH_3CN , $-\text{CH}_3$), 1.75 (s, 3H, CH_3CN , $-\text{CH}_3$). $^{31}\text{P}\{^1\text{H}\}$ -NMR (CD_2Cl_2 , 161MHz, δ in ppm): 51.98 (d, $J_{\text{P-P}} = 43.7\text{Hz}$), 51.13(d, $J_{\text{P-P}} = 43.7\text{Hz}$), -144.3 (sept, $J_{\text{P-F}} = 712.8\text{Hz}$, PF_6). $^{19}\text{F}\{^1\text{H}\}$ -NMR (CD_2Cl_2 , 376.8MHz, δ in ppm): -71.5 (d, 6F, $J_{\text{P-F}} = 712.8\text{Hz}$, PF_6). ESI-HRMS: Calculated for $\text{C}_{53}\text{H}_{49}\text{F}_{12}\text{FeN}_5\text{P}_2$: Exact: [M: 1163.2096, M - (CH_3CN) $_2(\text{PF}_6)_2$ /Z: 395.6136]; Experimental [M - (CH_3CN) $_2(\text{PF}_6)_2$ /Z: 395.6130]. Elemental Analysis: Calculated for $\text{C}_{53}\text{H}_{49}\text{F}_{12}\text{FeN}_5\text{P}_2 \cdot 3\text{CH}_2\text{Cl}_2$: C, 47.42; H, 3.91; N, 4.94; found C, 47.32; H, 3.21; N, 4.81.

General Procedure for the Asymmetric Transfer Hydrogenation of Ketones: In a typical experiment, inside the glovebox $\text{Fe}_3(\text{CO})_{12}$ (3.4 mg, 0.0068 mmol), (**2**) (5 mg, 0.0068 mmol) were placed in a tube equipped with a Teflon-coated magnetic stirring bar. Isopropyl alcohol (3 mL) was then added and the mixture was stirred at 70 °C for 30 min. An appropriate amount of KOH was then added, and the mixture was continually stirred for another 15 min. Ketone was then introduced and the mixture was stirred at 70 °C for the required reaction time. Conversion and enantiomeric ratios were calculated by GC using the ChirasilDex CB chiral column.

Procedure for the Asymmetric Transfer Hydrogenation of Isobutyrophenone in Presence of Mercury: $\text{Fe}_3(\text{CO})_{12}$ (3.4 mg, 0.0068 mmol), (**2**) (5 mg, 0.0068 mmol) were placed in a tube equipped with a Teflon-coated magnetic stirring bar. Isopropyl alcohol (3 mL) was then added and the mixture was stirred at 70 °C for 30 min. KOH (3.05 mg, 0.054 mmol) was then added, and the mixture was continually stirred for another 15 min. Isobutyrophenone (20.4 μL , 0.136 mmol) was then introduced and the mixture was stirred at 70 °C for 5 h. An aliquot was taken under N_2 and analyzed by GC using the ChirasilDex CB chiral column. At the same time, Hg was added to the reaction and left to stir at 70 °C for 10 h. After cooling down to room temperature, a sample was carefully taken from the top of the reaction mixture, the rest of which was quenched with sulfur and collected in a special bottle.

Computational Details: All calculations were performed using Gaussian 09.^[27] For $[\text{FeLL}'(\mathbf{2}_\mu)]$ complexes, B3LYP density functional was used and the basis set was SDD for iron atom (including relativistic core potentials) and 6-31++G(d,p) for Cl, P, N, O, C and H atoms. We used B97D density functional (which includes dispersion) for $[\text{FeCl}_2(\mathbf{2})]$ complex calculations and all atoms were treated with 6-31++G(d,p) all electron basis set. Solvent effects were included using the Polarizable Continuum Model (PCM) with the integral equation formalism variant (IEFPCM). Solvent was dichloromethane for bis(chloride) complex and acetone for acetonitrile complexes, CO and CH_3CN free molecules. Calculated structures were generated by J mol.^[28]

X-ray Crystallography: X-ray diffraction data for compounds **4** and **6** were collected at the X-ray diffraction beamline of synchrotron Elettra (Trieste) at 100(2) K, with $\lambda = 0.7000$ and 0.8000 Å, respectively. Cell refinement, indexing, and scaling of the data sets were carried out using the CCP4 software suite.^[29] Both the structures were solved by direct methods and refined by a full-matrix least-squares procedure based on F^2 using SHELXL-97.^[30]

The ΔF map revealed a molecule of CH_2Cl_2 (refined at half occupancy) in **4**, while a disordered pentane molecule and a residual refined as water (H atoms not fixed) were detected in the unit cell of **6**. All non-hydrogen atoms were refined anisotropically. The hydrogen atoms were placed at calculated positions and treated using the appropriate riding models. Crystal data and details of refinement are given in Supporting information.

CCDC 1941308 (for **4**), and 1941306 (for **6**) contain the supplementary crystallographic data for this paper. These data can be obtained free of charge from The Cambridge Crystallographic Data Centre.

Supporting Information (see footnote on the first page of this article): Associated details, product characterization data, crystallographic data for **4** and **6**, and ^1H , ^{13}C , ^{31}P , ^{11}B and ^{19}F spectra are available.

Acknowledgments

The authors are grateful to the Spanish Ministerio de Economía y Competitividad and the Fondo Europeo de Desarrollo Regional FEDER (PhD grant BES-2011-043510 to E. M., CTQ2016-75016-R, AEI/FEDER,UE), and the Generalitat de Catalunya (2017SGR) for financial support.

Keywords: Homogeneous catalysis · N,P ligands · Ligand design · Asymmetric catalysis

- [1] T. Ikariya, A. J. Blacker, *Acc. Chem. Res.* **2007**, *40*, 1300–1308.
- [2] a) H. Doucet, T. Ohkuma, K. Murata, T. Yokozawa, M. Kozawa, E. Katayama, A. F. England, T. Ikariya, R. Noyori, *Angew. Chem. Int. Ed.* **1998**, *37*, 1703–1707; *Angew. Chem.* **1998**, *110*, 1792; b) K. Junge, K. Schroder, M. Beller, *Chem. Commun.* **2011**, *47*, 4849–4859; c) R. M. Bullock, *Science* **2013**, *342*, 1054–1055; d) P. E. Sues, K. Z. Demmans, R. H. Morris, *Dalton Trans.* **2014**, *43*, 7650–7667; e) R. M. Bullock, Molybdenum and Tungsten Catalysts for Hydrogenation, Hydrosilylation and Hydrolysis, in *Catalysis without Precious Metals* (Wiley-VCH Verlag GmbH & Co. **2010**).
- [3] a) S. Enthaler, K. Junge, M. Beller, *Angew. Chem. Int. Ed.* **2008**, *47*, 3317–3321; *Angew. Chem.* **2008**, *120*, 3363; b) G. Bauer, K. A. Kirchner, *Angew. Chem. Int. Ed.* **2011**, *50*, 5798–5800; *Angew. Chem.* **2011**, *123*, 5918.
- [4] For a review on structural aspects of tri- and tetradentate P- and PN donor ligands, see: a) J. C. Hierso, R. Amardeil, E. Bentabet, R. Broussier, B. Gautheron, P. Meunier, P. Kalck, *Coord. Chem. Rev.* **2003**, *236*, 143–206; b) Y.-Y. Li, Z.-R. Dong, J.-X. Gao, *Curr. Top. Catal.* **2007**, *48*, 2587–2598.
- [5] T. L. Marxen, B. J. Johnson, P. V. Nilsson, L. H. Pignolet, *Inorg. Chem.* **1984**, *23*, 4663–4670.
- [6] J. C. Jeffery, P. A. Tucker, T. B. Rauchfuss, *Inorg. Chem.* **1980**, *19*, 3306–3316.
- [7] a) J. X. Gao, T. Ikariya, R. Noyori, *Organometallics* **1996**, *15*, 1087–1089; b) R. Noyori, S. Hashiguchi, *Acc. Chem. Res.* **1997**, *30*, 97–102; c) Y.-Y. Li, S.-L. Yu, W.-Y. Shen, J.-X. Gao, *Acc. Chem. Res.* **2015**, *48*, 2587–2598.
- [8] a) R. Bigler, E. Otth, A. Mezzetti, *Organometallics* **2014**, *33*, 4086–4099; b) R. Bigler, A. Mezzetti, *Org. Lett.* **2014**, *16*, 6460–6463; c) R. Bigler, R. Huber, A. Mezzetti, *Angew. Chem. Int. Ed.* **2015**, *54*, 5171–5174; *Angew. Chem.* **2015**, *127*, 5260; d) L. De Luca, A. Mezzetti, *Angew. Chem. Int. Ed.* **2017**, *56*, 11949–11953; *Angew. Chem.* **2017**, *129*, 12111.
- [9] S. Zhou, S. Fleischer, K. Junge, S. Das, D. Addis, M. Beller, *Angew. Chem. Int. Ed.* **2010**, *49*, 8121–8125; *Angew. Chem.* **2010**, *122*, 8298.
- [10] a) C. Sui-Seng, F. Freutel, A. J. Lough, R. H. Morris, *Angew. Chem. Int. Ed.* **2008**, *47*, 940–943; *Angew. Chem.* **2008**, *120*, 954; b) N. Meyer, A. J. Lough, R. H. Morris, *Chem. Eur. J.* **2009**, *15*, 5605–5610; c) C. Sui-Seng, F. N. Haque, A. Hadzovic, A. M. Pütz, V. Reuss, N. Meyer, A. J. Lough, M. Zimmer-De Iulii, R. H. Morris, *Inorg. Chem.* **2009**, *48*, 735–743; d) A. Mikhailine, A. J. Lough, R. H. Morris, *J. Am. Chem. Soc.* **2009**, *131*, 1394–1395.
- [11] A. A. Mikhailine, M. I. Maishan, R. H. Morris, *Org. Lett.* **2012**, *14*, 4638–4641.
- [12] For selected examples see: a) P. O. Lagaditis, A. J. Lough, R. H. Morris, *J. Am. Chem. Soc.* **2011**, *133*, 9662–9665; b) D. E. Prokopchuk, J. F. Sonnenberg, N. Meyer, M. Zimmer-De Iulii, A. J. Lough, R. H. Morris, *Organometallics* **2012**, *31*, 3056–3064; c) D. E. Prokopchuk, R. H. Morris, *Organometallics* **2012**, *31*, 7375–7385.
- [13] a) A. A. Mikhailine, E. Kim, C. Dingels, A. J. Lough, R. H. Morris, *Inorg. Chem.* **2008**, *47*, 6587–6589; b) A. A. Mikhailine, R. H. Morris, *Inorg. Chem.* **2010**, *49*, 11039–11044.
- [14] a) P. O. Lagaditis, A. L. Lough, R. H. Morris, *Inorg. Chem.* **2010**, *49*, 10057–10066; b) P. E. Sues, A. J. Lough, R. H. Morris, *Organometallics* **2011**, *30*, 4418–4431.
- [15] J. F. Sonnenberg, N. Coombs, P. A. Dube, R. H. Morris, *J. Am. Chem. Soc.* **2012**, *134*, 5893–5899.
- [16] A. A. Mikhailine, M. I. Maishan, A. J. Lough, R. H. Morris, *J. Am. Chem. Soc.* **2012**, *134*, 12266–12280.
- [17] a) W. Zuo, A. J. Lough, Y. F. Li, R. H. Morris, *Science* **2013**, *342*, 1080–1083; b) K. Z. Demmans, C. S. G. Seo, A. J. Lough, R. H. Morris, *Chem. Sci.* **2017**, *8*, 6531–6541.
- [18] V. Rautenstrauch, X. Hoang-Cong, R. Churlaud, K. Abdur-Rashid, R. H. Morris, *Chem. Eur. J.* **2003**, *9*, 4954–4967.
- [19] W. Baratta, F. Benedetti, Z. A. Del, L. Fanfoni, F. Felluga, S. Magnolia, E. Putignano, P. Rigo, *Organometallics* **2010**, *29*, 3563–3570.
- [20] J. Skarzewski, A. Gupta, *Tetrahedron: Asymmetry* **1997**, *8*, 1861–1867.
- [21] a) J. Zhang, M. Gandelman, D. Herrman, G. Leitus, L. J. W. Shimon, Y. Ben-David, D. Milstein, *Inorg. Chim. Acta* **2006**, *359*, 1955–1960; b) B. M. Schmiede, M. J. Carney, B. L. Small, D. L. Gerlach, J. A. Halfen, *Dalton Trans.* **2007**, 2547–2562; c) T. Zell, R. Langer, M. A. Iron, L. Konstantinovskii, L. J. W. Shimon, Y. Diskin-Posner, G. Leitus, E. Balaraman, Y. Ben-David, D. Milstein, *Inorg. Chem.* **2013**, *52*, 9636–9649.
- [22] J.-S. Chen, L.-L. Chen, Y. Xing, G. Chen, W.-Y. Shen, Z.-R. Dong, Y.-Y. Li, J.-X. Gao, *Acta Chim. Sin.* **2004**, *62*, 1745–1750.
- [23] J. F. Sonnenberg, R. H. Morris, *Catal. Sci. Technol.* **2014**, *4*, 3426–3438.
- [24] Y. Li, S. Yu, X. Wu, J. Xiao, W. Shen, Z. Dong, J. Gao, *J. Am. Chem. Soc.* **2014**, *136*, 4031–4039.
- [25] J. A. Widegren, R. Finke, *J. Mol. Catal. A* **2003**, *198*, 317–341.
- [26] D. D. Perrin, W. L. F. Armarego, *Purification of Laboratory Chemicals* (3rd ed., Pergamon Press, Oxford, **1989**).
- [27] M. J. Frisch, G. W. Trucks, H. B. Schlegel, G. E. Scuseria, M. A. Robb, J. R. Cheeseman, G. Scalmani, V. Barone, B. Mennucci, G. A. Petersson, H. Nakatsuji, M. Caricato, X. Li, H. P. Hratchian, A. F. Izmaylov, J. Bloino, G. Zheng, J. L. Sonnenberg, M. Hada, M. Ehara, K. Toyota, R. Fukuda, J. Hasegawa, M. Ishida, T. Nakajima, Y. Honda, O. Kitao, H. Nakai, T. Vreven, J. A. Montgomery Jr., J. E. Peralta, F. Ogliaro, M. Bearpark, J. J. Heyd, E. Brothers, K. N. Kudin, V. N. Staroverov, R. Kobayashi, J. Normand, K. Raghavachari, A. Rendell, J. C. Burant, S. S. Iyengar, J. Tomasi, M. Cossi, N. Rega, J. M. Millam, M. Klene, J. E. Knox, J. B. Cross, V. Bakken, C. Adamo, J. Jaramillo, R. Gomperts, R. E. Stratmann, O. Yazyev, A. J. Austin, R. Cammi, C. Pomelli, J. W. Ochterski, R. L. Martin, K. Morokuma, V. G. Zakrzewski, G. A. Voth, P. Salvador, J. J. Dannenberg, S. Dapprich, A. D. Daniels, Ö. Farkas, J. B. Foresman, J. V. Ortiz, J. Cioslowski, D. J. Fox, *Gaussian 09, Revision D.01*, Gaussian, Inc., Wallingford CT, **2009**.
- [28] Jmol: an open-source Java viewer for chemical structures in 3D. <http://www.jmol.org/>.
- [29] Collaborative Computational Project, Number 4, *Acta Crystallogr., Sect. D* **2011**, *67*, 235–242.
- [30] G. M. Sheldrick, *Acta Crystallogr., Sect. A* **2008**, *64*, 112–122.

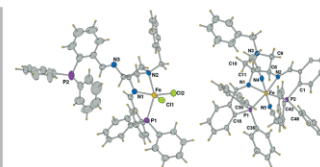
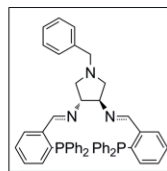
Received: July 18, 2019

Asymmetric Transfer Hydrogenation

E. Mercadé, E. Zangrando, A. Clotet, C. Claver, C. Godard** 1–11



Novel Chiral PNNP Ligands with a Pyrrolidine Backbone – Application in the Fe-Catalyzed Asymmetric Transfer Hydrogenation of Ketones



PNNP ligands containing a pyrrolidine backbone were prepared and their coordination chemistry to iron was investigated through experimental and DFT studies. When used in combination with $\text{Fe}_3(\text{CO})_{12}$ as iron source in the

asymmetric transfer hydrogenation of ketones, the compounds afforded conversions higher than 95 % and enantioselectivities up to 97 % were achieved.

DOI: 10.1002/ejic.201900778